



International Congress of Science and Technology of Metallurgy and Materials, SAM - CONAMET 2013

Rapid Synthesis of Nanometric Cellulose Hydroxyapatite

Mónica Barberá de Estrella^{(1)*}, Sonia Torres de Flores⁽¹⁾, Norberto A. Bonini⁽¹⁾, Elio Gonzo⁽²⁾, Natalia P. Pérez⁽¹⁾ and Analía Natalí Arias⁽¹⁾

⁽¹⁾Facultad de Ciencias Exactas de la Universidad Nacional de Salta, Avda Bolivia 5150, Salta, Argentina

⁽²⁾Instituto Nacional de Investigación para la Industria Química, Avda Bolivia 5150, Salta, Argentina.

Abstract

Cellulose hydroxyapatite (Cel-HAp) nanometrics were prepared by microwave-assisted method in order to improve structural and morphological characteristics. The preparation of nanometric Cel-HAp was performed using different grades of cellulose (pharmaceutical aid and analytical reagent), $\text{CaCl}_2 \cdot 4\text{H}_2\text{O}$ and $\text{NaH}_2\text{PO}_4 \cdot 2\text{H}_2\text{O}$ precursors. The mixture was heated in a microwave oven at low temperatures (70°C and 90°C) for five minutes. This method is applied in order to reduce synthesis time as well as to obtain materials more efficient to remove pollutant ions. The solids were characterized by Electronic Spectroscopy (DRUV), X-rays diffraction, Vibrational Spectroscopy (FTIR, Raman) and SEM. FTIR and Raman spectra show the characteristic bands of carbonated hydroxyapatite and cellulose. X-rays diffraction shows the typical diffraction peaks of HAp and Cellulose. SEM shows morphological differences between obtained solids: spicular (Cel_A-HAp, analytical reagent) and stacked layers (Cel_F-HAp, pharmaceutical aid) respectively. From the SEM studies and applying Scherrer's formula the materials were found to be nanometrics

© 2015 The Authors. Published by Elsevier Ltd. This is an open access article under the CC BY-NC-ND license

(<http://creativecommons.org/licenses/by-nc-nd/4.0/>).

Selection and peer-review under responsibility of the scientific committee of SAM - CONAMET 2013

Keywords: Hydroxyapatite; Cellulose-Synthesis; Nanomaterials; Characterization; Microwave.

1. Introduction

Hydroxyapatite (HAp) which is represented by the formula $(\text{Ca})_{10}(\text{OH})_2(\text{PO}_4)_2$ is recognized bioceramic material due to its biocompatibility, meaning that it will form excellent chemical bonds with hard tissues and effective osteoconductivity. HAp has been produced by different processes of synthesis and precursors of calcium and phosphorus. Variations in processing techniques lead materials with some differences in structure and morphology.

Cellulose is a natural material, non-toxic, renewable, biodegradable and with readily modifiable properties. The preparation of cellulose-hydroxyapatite includes this polymer to HAp and result a material combining the advantages of cellulose and HAp. This compound Cel-HAp with nanometric particles sizes increases specific surface area and converts itself in a potential adsorbent material, as such can be used for removal process of pollution ions, for example it removes aqueous arsenate [1] and arsenite anions. Its characteristics non-toxic and biocompatibility are considered of interest in biomedical applications.

In this work, we applied a facile and fast route for here synthesis of HAp reported [1], which includes treatment at low temperature ($T < 100^\circ$). The utilization of microwave oven permits uniform heating of reactant system, this minimizes temperature gradients, reduce diffusion time of particles and we can obtain the product in short time [2,3]. So, small particle size and narrow size distribution can be obtained.

Nomenclature

HAp	hydroxyapatite
Cel-HAp	cellulose hydroxyapatite
Cel _F -HAp	cellulose-hydroxyapatite (pharmaceutical aid)
Cel _A -HAp	cellulose-hydroxyapatite (analytical quality)

2. Experimental process / methods

2.1. Cellulose-hydroxyapatite synthesis

Cel_F-HAp and Cel_A-HAp are obtained, from alkalines cellulose solutions, of pharmaceutical use and analytical quality, respectively. Each of the alkalines solutions are prepared to add sodium hydroxide and urea, with vigorous stirring and cooling at 0°C . Then, $\text{CaCl}_2 \cdot 4\text{H}_2\text{O}$ and NaH_2PO_4 solutions (Cicarelli reagent grade and distilled boiled water to avoid carbonate contamination) were added as precursors of calcium and phosphorus. The resultant mixture was vigorously stirred and it heated in microwave oven Coventry, to 70°C and 90°C , respectively, during 5 minutes. The product was cooled, separated from the solution by centrifugation to 3600 rpm during 5 minutes and washed with distilled boiled water and ethanol. Finally synthesized material was dried in heater at 60°C in heater during all the night.

2.2. Cellulose-hydroxyapatite characterization

The structural characterizations of materials were investigated by using the following structural and morphology studies: a) UV diffuse reflectance (DRUV) realized in GBC Cintra 10e UV-Visible Spectrophotometer with integration sphere, b) Infrared (FTIR) and Raman with Spectrum G-X Perkin Elmer spectrometer, c) X-ray diffractometry (XRD) with Rigaku Miniflex X-Ray Diffractometer System diffractometer, d) The solids morphology were studied by Scanning Electron Microscopy (SEM) with electron microscope JEOL Model JSM 6480LV, e) The crystal grain size of the crystalline fraction of the samples was calculated applying Scherrer formula for hydroxyapatite cellulose[4].

3. Results and discussion

3.1. Diffuse reflectance UV spectra

The sample was conveniently ground, spread on filter paper (sample support) with a spatula and fixed in the sampling accessory. In Fig. 1) a) y 1)b) show the spectra corresponding to the two types of cellulose, Cel_A-HAp, Cel_F-HAp and filter paper. Comparing the peaks of cellulose and phosphate in both materials and filter paper. Both Cel-HAp (Fig. 1) shows the charge transfer phosphate band (approximately 320 nm) 20 nm around displaced respect to hydroxyapatite [5] and the band corresponding to cellulose (approximately 220 nm), also they have a

displacement respect to the free cellulose (approximately 210 nm) (Fig. 1). Bathochromic shifts indicate the influence the effect of the interaction between the phosphate groups and cellulose.

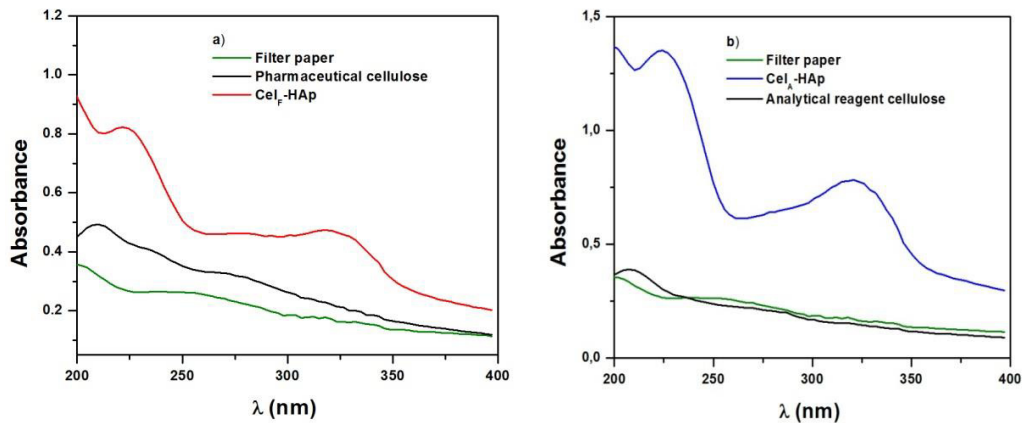


Fig.1. Diffuse reflectance UV spectra. a) Cel_F-HAp (red line), Pharmaceutical cellulose (solid black line), filter paper (green line). b) . Cel_A-HAp (blue line), analytical reagent cellulose (black line), filter paper (green line)

3.2. Infrared spectra: Plotted frequency versus absorbance (cm^{-1})

A tablet was prepared by dispersing of the sample in KBr, previously dried in a vacuum oven. Three samples of hydroxyapatite were studied; two samples were prepared using analytical quality cellulose (Cel_A-HAp) and pharmaceutical cellulose excipient (Cel_F-HAp), and the third sample, hydroxyapatite (HAp) was obtained by the conventional precipitation method. The resulting spectra are shown in Figures 2 to 5. The spectra of figure 2 and 3, corresponding to HAp, Cel_A-HAp and Cel_F-HAp (the last two synthesized at different temperatures), were compared. It was observed that the profile of signals corresponding to the hydroxyapatite was maintained but with some modifications in areas where solid signals are overlapped with those for cellulose [2] (band at 2903 cm^{-1} was assigned to asymmetrically stretching vibration of C-H in pyranoid ring). Example: highlights the broad band corresponding to OH-, at 3500 cm^{-1} of cellulose, which overlaps the peak of the same group but corresponding to the spectra hydroxyapatite, the same happens with the band corresponding to asymmetric (ν_3 : $1100\text{-}1022 \text{ cm}^{-1}$) and symmetric stretching (ν_1 : 959 cm^{-1}) [6,7] of phosphate, the first is widens and it loses definition, and the second peak becomes a shoulder. A comparison of the spectra in figures 5 and 6 (corresponding to cellulose and Cellulose-HAp materials) together with the HAp spectrum (showed in figure 3), shows a strong interaction between HAp and cellulose. In all spectra of Cel_A-HAp, Cel_F-HAp and HAp the bands for CO_3^{2-} are notable, in the spectra of the composite hydroxyapatite is observed a band at 1660 cm^{-1} corresponding to stretching vibration of superficial carbonate. The superficial carbonate plays an important role in reducing the size of the crystal grains in the scale nanometric of biological and non-biological apatites [8]. There are no significant differences between the materials obtained at different temperatures or between the Cel-HAp prepared with cellulose of different qualities.

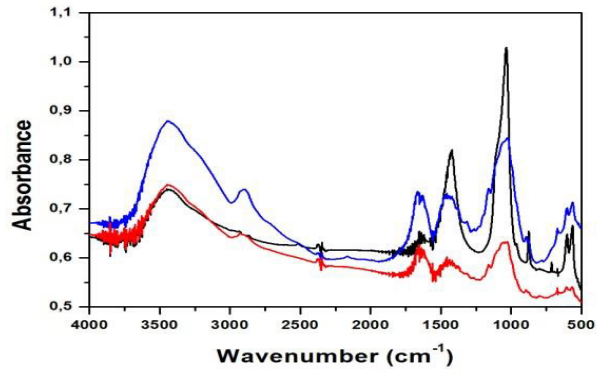


Fig.2. Infrared spectra. Hap (black line), Cel_A-HAp (blue line), Cel_F-HAp (red line), Temperature= 90°C

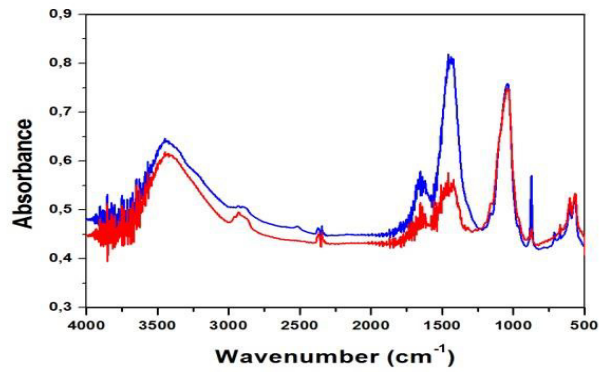


Fig.3. Infrared spectra. Cel_A-HAp (blue line) y Cel_F-HAp (red line), Temperature=70°C

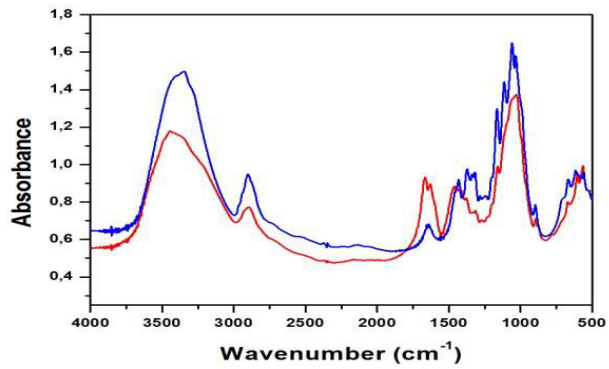


Fig.4. Infrared spectra. Cel_F-HAp(red line) (temperature= 90°C) and pharmaceutical cellulose (blue line)

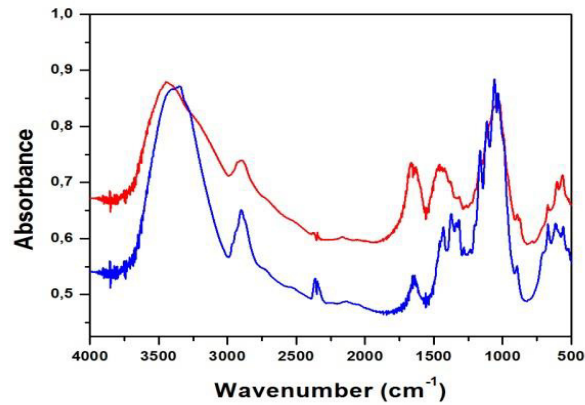


Fig.5. Infrared spectra. Cel_A-HAp (red line) (Temperature= 90°C) and analytical quality cellulose (blue line)

3.3. Raman Spectra: Plotted signal intensity versus frequency (cm^{-1})

Raman spectra: nanocomposite samples were irradiated contained in a capillary tube and increased dwell time in order to minimize the emission of fluorescence. (Exception: the spectra obtained from the two pulps used for comparative purposes). Laser Wavelength: 1064 microns (near infrared.) Is a nondestructive spectroscopic method [9 to 12], which identifies different phases present in the sample [9, 10]. The assignments of the Raman bands are arranged in Table 1.

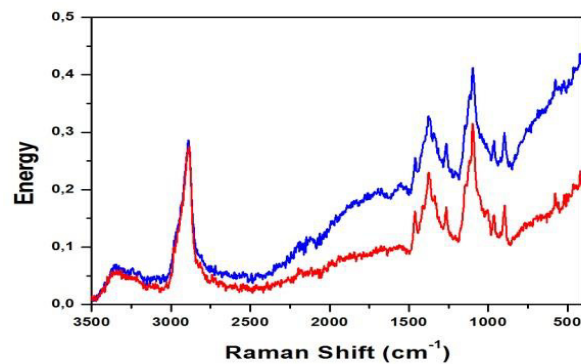


Fig. 6. Raman Spectra. Cel_E-HAp (red line), Cel_A-HAp (blue line). Temperature: 70°C

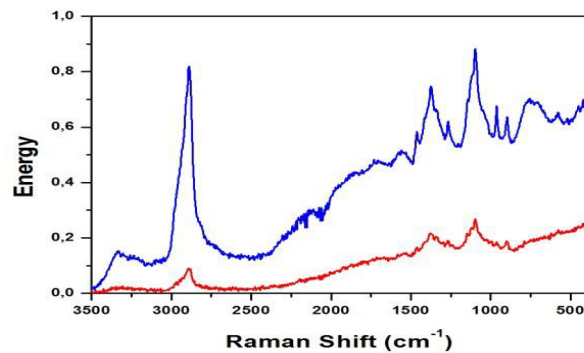


Fig.7. Raman Spectra .Cel_E-HAp (red line), Cel_A-HAp (blue line) a 90°C

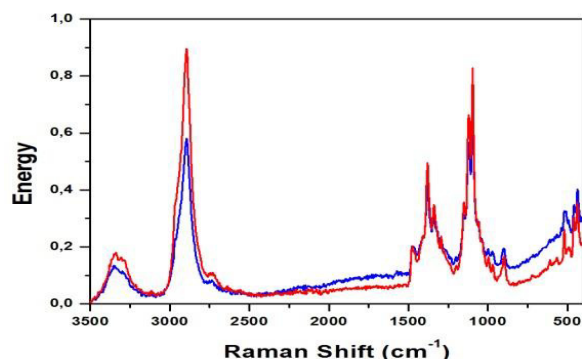


Fig. 8. Raman Spectra. Pharmaceutical cellulose (red line), Analytical quality cellulose (blue line).

The assignments of the bands to cellulose and HAp are shown in Table 1. No significant differences in the spectroscopic signals to celluloses, used to prepare composite materials, or in the Cel-HAp obtained. No influence of temperature variation. Assignments of experimental data were extracted from the literature, so that the exact position of the bands may differ due to the different calibration of the equipment. Most of the vibrational modes are highly coupled and delocalized. In the case of cellulose, pyranoid rings and the links between them consist of C-C and C-O bonds it have similar reduced masses and binding energies [12].

Table 1. Spectra Raman Assignment

Phase	Frequency (cm ⁻¹)	Assignments	Intensity
Cellulose	3300	Stretching group OH	Medium intensity broad band
	2890	Stretching vibrations of methylene and methine groups	Sharp and intense peak
	1380	Deform. HCC-HCO- COH-CH ₂ (combination band)	Very strong
	1083	Deform. glycosidic COC + symmetric stretching corresponding to the pyranoid ring breathing	
	898	Related to the degree of disorder crystalline cellulose (lattice type II) [10]	Sharp peak
PO ₄ ³⁻ (T _d)	962	Stretching of tetrahedron PO ₄ ³⁻ symmetric	Sharp and low intensity peak
	400-490	Deformation O-P-O	
	570-625	Deformation O-P-O	
	1020-1095	Asymmetric stretching P-O	

3.4. X-ray diffraction pattern

Materials were treated at different temperatures. In the diffraction pattern are observed cellulose ($2\theta = 20^\circ, 21.6^\circ$) and hydroxyapatite peaks ($2\theta = 25.8^\circ, 31.9^\circ, 32^\circ, 34^\circ$). The signals corresponded to low solid crystal characteristics and showed that by increasing the synthesis temperature the relation between the signal intensities of cellulose and hydroxyapatite is changed, increasing the first in the Cel-HAp obtained at 90°C and also had a little improvement in the crystalline characteristics.

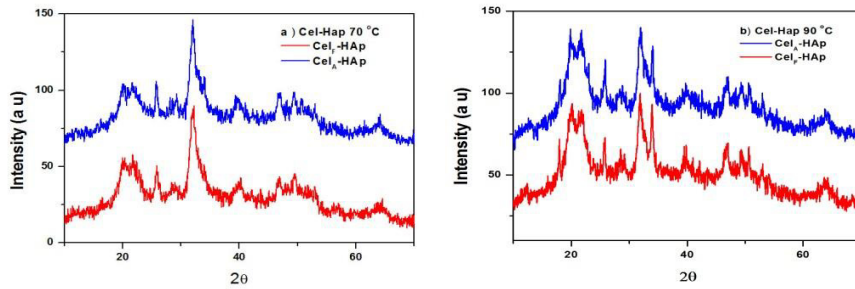


Fig. 9.XRD patterns: a) Cel_F-HAp (red line), Cel_A-HAp (blue line), b) Cel_F-HAp (red line), Cel_A-HAp (blue line)

3.4.1 Crystal grain size calculate on samples treated of cellulose-hydroxyapatite at 90°C

Scherrer formula was used for this purpose, choosing the index Miller peak (002), because it is the only peak which does not overlaps with others, and it is a size index of crystallographic c axis. The results of this calculation are shown in Table 2.

$$\text{Crystalline grain size} = \frac{0,9 \lambda}{\beta \cdot \cos\theta}$$

Where:

λ: X ray monochromatic wavelength corresponding to Cu line (0, 15408 nm)

0.9: Constant value

β: (FWHM): peak width at height half (expressed in radians)

θ : Diffraction angle half

Table 2. Crystalline sizes calculated are of the order nanometric and smaller than the HAp.			
Samples	θ(°)	B	Size crystalline (c direction)/nm
Cel _A -Hap	12.9	0.005496	26
Cel _F -Hap	12.9	0.005496	26
HAp	12.9	0.005496	38

3.6. Scanning Electron Microscopy

The particles were gold coated the resulting SEM images, for different samples, are shown in Fig.10 to 12. Fig.10 shows the particle size distribution of HAp powders synthesized by precipitation method and treated at 100°C. Fragments are observed with small micron or submicron aggregates. The figure highlights the material porosity.

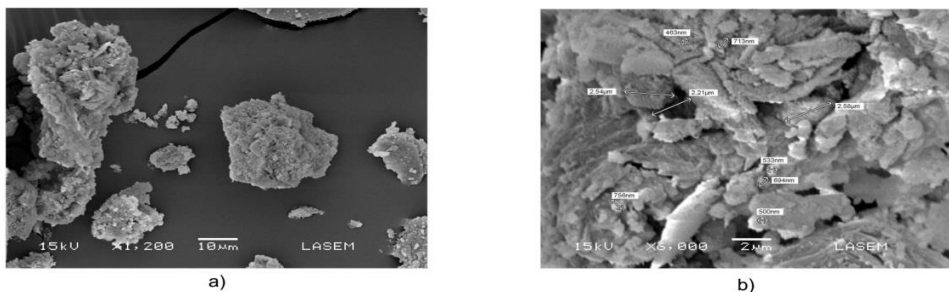


Fig. 10. SEM images of HAp synthesized via precipitation method and heat treated at 100°C. a) agglomerate of the HAp powder; b) details of the HAp powder.

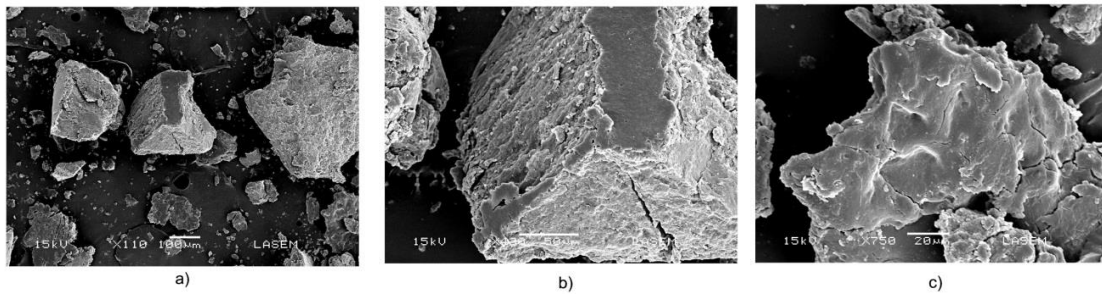


Fig.11. SEM images of Cel_F-HAp powder. a) agglomerate of Cel_F-HAp powder; b-c) details of the Cel_F-HAp powder.

The morphology of Cel_A-HAp powder is shown in Fig.12. With a major magnification, Fig.12.b-d); plates with a spicular arrangement and thickness are observed, which sets it apart from the Cel_F-HAp. The synthesis temperature does not change the morphology

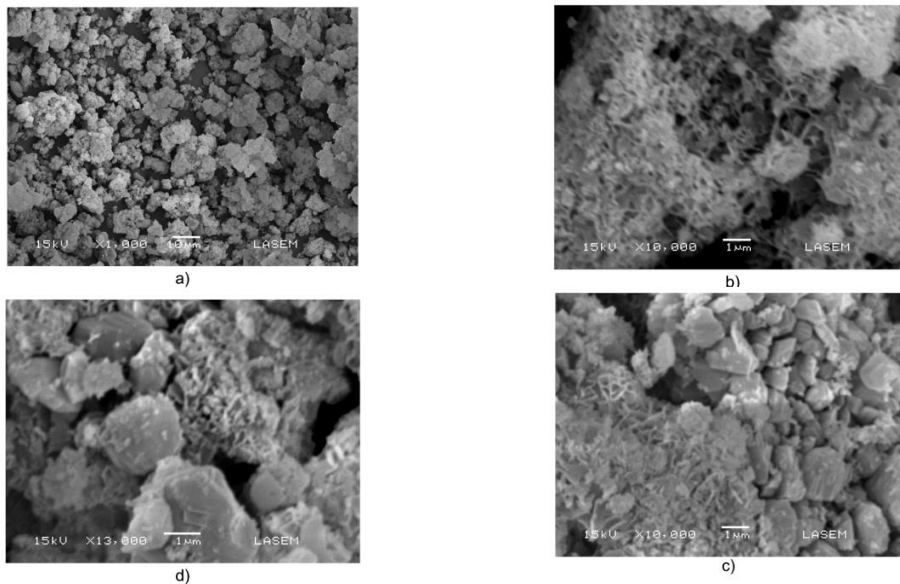


Fig.12. SEM images of Cel_A-HAp powder. a) agglomerate of Cel_A-HAp powder; b-c-d) details of the Cel_A-HAp powder.

So, in the SEM images are detected morphological differences between the solid without cellulose (HAp) and those with cellulose (Cel_A-HAp, Cel_F-HAp) and between the latter, characterized by layers or sheets but arranged differently, indicating the influence of the cellulose quality used in preparation

4. Conclusions

FTIR, Raman and Diffuse Reflectance spectra of the cellulose and the hydroxyapatite are modified in the composite material indicating strong interactions of cellulose polymer with the inorganic phosphate matrix corresponding (hydrogen bridges links). There are not significant differences in spectroscopic signals of celluloses used to prepare composite materials, or in the Cel-HAp obtained, it did not influence the temperature variation.

Diffraction patterns show that the composites hydroxyapatite fitted to diffraction pattern of hydroxyapatite, but low definition of the peaks revealed that is a material of scarce crystallinity. Calculating the particle size of the crystal grain indicated that is a solid nanometric dimension (was only calculated for the case of 90°C, by lack of data from treated material at 70°C due to a lower crystal growth).

Morphological aspects (SEM) are different when working with cellulose purity greater compared to the commercial product. It is likely that the differences were due to the polymerization degree and hence the different molecular weight of both polymers. There is not influence of temperature. That highlights the influence of the cellulose in the hydroxyapatite morphology.

Through a simple and rapid method -using the microwave oven- is achieved synthesize a composite material of cellulose hydroxyapatite, whose structure, crystallinity and morphology are confirmed by FTIR, Raman, XRD and SEM. The low crystallinity related to the high content of carbonate and nanometric size particles, promotes high chemical reactivity that can result in a potential adsorbent of contaminant ions.

Results concluded that Cel-HAp was obtained, operating at 70°C ($T < 90^\circ$). On the other hand the type of cellulose to be used in the synthesis allowed modifying the morphology of the hydroxyapatite.

5-References

- [1] Mahamudur I. et al. Arsenate removal from aqueous solution by cellulose-carbonated hydroxyapatite nanocomposites. *J. Hazard. Mat.* Vol. 189, (2011) p. 755-763.
- [2] Jingbing L. et al. Rapid formation of hydroxyapatite nanostructures by microwave irradiation. *Chem. Phys. Lett.* Vol. 396(4-6), (2004) p. 429-432.
- [3] Ning Jia et al. Microwave-assisted synthesis and characterization of cellulose – carbonated hydroxyapatite nanocomposites in NaOH-urea aqueous solution. *Mat. Lett.* Vol.64, (2010) p. 2223-2225.
- [4] Salimi M. N. et al. Effect of processing conditions on the formation of hydroxyapatite nanoparticles. *Powder Technol.* Vol.218, (2012) p. 109-118.
- [5] De la Orden M. U. et al. Effect of different coupling agents on the browning of cellulose polypropylene composites during melt processing. *Polymer. Degrad. Stabil.* 95 (2010) 201- 206.
- [6] Murugan R. et al. Crystallographic Studies Derived from Various Sources. *Crystal Growth & Design.* Vol. 5(1), (2005). p. 111-112.
- [7] Śosarczyk Ana et al. (2004). FTIR and XRD evaluation of carbonated hydroxyapatite powders synthesized by wet methods. *J. Mol. Struct.* Vol. 744-747, p.657-661.
- [8] Wopenka Brigitte et al. A mineralogical perspective on the apatite in bone. *Mat. Sci. and Eng. C* Vol.25 (2), (2005).p.131-143.
- [9] Cuscó, R. et al. Differentiation between hydroxyapatite and β -TCP by means of μ -Raman spectroscopy. *Journal of the European Ceramic Society.* Vol. 18(9), (1998) p. 1301-1305.
- [10] Darimont G. L. et al. Non-destructive evaluation of crystallinity and chemical composition by Raman spectroscopy in hydroxyapatite-coated implants. *Mat. Lett.* Vol.58, (2003) p.71-73.
- [11] Kavkler K. et al. Examination of cellulose fibres in historical objects by micro Raman spectroscopy. *Spectrochim. Acta A* Vol.78, (2011) p. 740-746.
- [12] Silva C.C. et al. Raman spectroscopy measurements of hydroxyapatite obtained by mechanical alloying. *J. Phys. Chem. Solids* Vol.65, (2004). p. 1031-1033.